

# EUROPHYSICS LETTERS

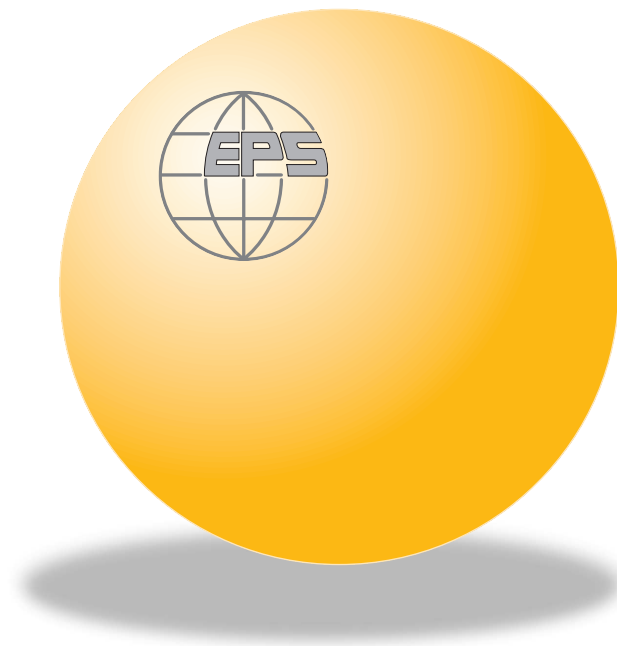
OFFPRINT

Vol. 71 • Number 3 • pp. 466–472

**Detection of synchronization for non-phase-coherent  
and non-stationary data**

\* \* \*

M. C. ROMANO, M. THIEL, J. KURTHS, I. Z. KISS and J. L. HUDSON



Published under the scientific responsibility of the  
**EUROPEAN PHYSICAL SOCIETY**  
Incorporating  
JOURNAL DE PHYSIQUE LETTRES • LETTERE AL NUOVO CIMENTO



## Detection of synchronization for non-phase-coherent and non-stationary data

M. C. ROMANO<sup>1</sup>, M. THIEL<sup>1</sup>, J. KURTHS<sup>1</sup>, I. Z. KISS<sup>2</sup> and J. L. HUDSON<sup>2</sup>

<sup>1</sup> *Institute of Physics, University of Potsdam  
Am Neuen Palais 10, 14469 Potsdam, Germany*

<sup>2</sup> *Department of Chemical Engineering, University of Virginia  
102 Engineers Way, Charlottesville, VA 22904-479, USA*

received 17 March 2005; accepted in final form 6 June 2005

published online 6 July 2005

PACS. 82.40.Bj – Oscillations, chaos, and bifurcations.

PACS. 83.85.Ns – Data analysis (interconversion of data computation of relaxation and retardation spectra; time-temperature superposition, etc.).

**Abstract.** – We present a new method to detect phase as well as generalized synchronization in a wide class of complex systems. It is based on the recurrences of the system's trajectory to the neighborhood of a former state in phase space. We illustrate the applicability of the algorithm for the paradigmatic chaotic Rössler system in the funnel regime and for noisy data, where other methods to detect phase synchronization fail. Furthermore, we demonstrate for electrochemical experiments that the method can easily detect phase and generalized synchronization in non-phase-coherent and even non-stationary time series.

*Introduction.* – Synchronization of chaotic systems has been extensively studied in the last years. There are three main types: complete synchronization (CS) [1], generalized synchronization (GS) [2–4] and phase synchronization (PS) [5, 6] (and lag synchronization (LS) as a special case of GS [7, 8]). All have applications in many different fields [9–12]. In this paper we concentrate on the detection of PS and GS in time series. Two systems are said to be phase synchronized when the difference of their respective phases is bounded. If the system has a dominant peak in the power spectrum, there are several methods to define the phase. One possibility is to project the trajectory on an appropriate plane, so that the projection looks like a smeared limit cycle with well-defined rotations around a center. Then the phase is identified with the angle of rotation [5, 6]. Another possibility is to apply the analytical signal approach [5, 6]. But a pre-requisite for the appropriate application of these techniques is that the trajectories in the projection plane go around an origin. This may be violated if the signal has a broad-band spectrum, which is typical for non-coherent signals [5, 6, 13]. For some chaotic systems it is possible to choose a Poincaré surface that is crossed transversally by all trajectories. Then, the phase is defined as a linear function of time, which increases by  $2\pi$  with each return to the surface of section. But for rather complex signals it is very hard or even impossible to find a section surface that is crossed transversally by each trajectory embedded in the attractor [5, 6]. Recently, another definition of the phase, based on the general idea of curvature, has been proposed to treat such systems, *e.g.*, the Rössler system in the non-coherent funnel regime [14]. However, this approach is in general limited to lower-dimensional systems. Hence, the open question is how to detect PS in the case of general non-coherent or complex signals.

In this letter we propose an approach to detect PS as well as GS based on the recurrences of the trajectory of a dissipative chaotic system in phase space, which is applicable to a wide class of chaotic systems and even for time series corrupted by noise, where other methods proposed so far fail. The concept of recurrences in dynamical systems goes back to Poincaré [15], when he proved that after a sufficiently long time interval, the trajectory of a dynamical system will return arbitrarily close to each former point of its route with probability one. Much later, recurrence plots (RPs) were introduced to yield a visual representation of recurrences in phase space [16]. We have recently shown that all relevant topological information about the underlying system is contained in the RP [17, 18]. RPs are defined for a given trajectory  $\{\mathbf{x}_i\}_{i=1}^N$ , with  $\mathbf{x}_i \in \mathcal{R}^n$  of a dynamical system and are based on the matrix

$$R_{i,j}^{(\varepsilon)} = \Theta(\varepsilon - \|\mathbf{x}_i - \mathbf{x}_j\|), \quad i, j = 1, \dots, N, \quad (1)$$

where  $\varepsilon$  is a predefined threshold and  $\Theta(\cdot)$  is the Heaviside function. Then the value “1” is coded as a black dot and the value “0” as a white dot in the plot. Hence, one obtains an  $N \times N$  matrix which provides a visual impression of the system behavior.

*Detection of PS.* – Using eq. (1) we define the phase  $\Phi$ : in periodic systems, the phase increases by  $2\pi$  when the trajectory completes one rotation around the center or, equivalently, when  $\|\mathbf{x}(t+T) - \mathbf{x}(t)\| = 0$ , where  $T$  is the period. For complex systems we assign an increment of  $2\pi$  to the phase when  $\|\mathbf{x}(t+\tau) - \mathbf{x}(t)\| \sim 0$ , or here when  $\|\mathbf{x}(t+\tau) - \mathbf{x}(t)\| < \varepsilon$ . That means a black point in the RP at the coordinates  $(t, t + \tau)$  can be interpreted as an increment of  $2\pi$  for the phase in the time interval  $\tau$  (of course,  $\tau$  must be greater than the correlation time of the system, or, equivalently, greater than the Theiler window [19]). In this way, we do not need to define a plane, onto which the trajectory is projected. We avoid the problem present in the analysis of non-coherent oscillators of finding an origin around which all points of the projected trajectory oscillate. Another problem linked to the definition of the phase based on a projection on a plane, is the appearance of false neighbors. For example, projecting a purely periodic trajectory lying in a 3-dimensional Cartesian space, can lead to intersections of the projected trajectory, and hence to ambiguity in the choice of the origin. Using the recurrence approach we avoid this problem as well because we consider the trajectories of the untangled attractor and hence we have no false neighbors. Note that the RP approach is different from the Poincaré section approach because no section surface has to be defined. We define a recurrence as the return of the trajectory to a former visited neighborhood and not as the transversal cross of a predefined plane. Furthermore, a chaotic trajectory switches from one unstable periodic orbit (UPO) to another and we find a recurrence every time the trajectory has completed a turn around one UPO. Such a recurrence corresponds to an increment of  $2\pi$  for  $\Phi$  in the original phase space, but not necessarily on the projection. When two chaotic oscillators are in PS their UPOs are locked [5, 6]. Hence, using the RP-based phase, there exists a  $n_i : m_i$  relationship between the phases, where  $i$  denotes a time index. This is because the UPOs that synchronize have in general different periods. However, it is cumbersome to compute a statistic that quantifies the instantaneous  $n_i\Phi_1 = m_i\Phi_2$  relationship between the phases, because  $n_i$  and  $m_i$  depend on time and the RP-based phase depends on  $\varepsilon$ . This drawback can be overcome by computing a statistical measure on how often  $\Phi_1$  and  $\Phi_2$  increase by  $2\pi$  or multiples of  $2\pi$  within the time interval  $\tau$ . If two systems are in PS, the “RPs-phases” of both systems increase in average  $2\pi k$ , with  $k$  a natural number, within the same time interval  $\tau$ . Therefore, looking at the probability  $P^{(\varepsilon)}(\tau)$  that the system returns to the  $\varepsilon$ -neighborhood of a former point  $\mathbf{x}_i$  of the trajectory after  $\tau$  time steps and comparing  $P^{(\varepsilon)}(\tau)$  for both systems allows to detect and quantify PS properly.  $P^{(\varepsilon)}(\tau)$  can be estimated

directly from the RP as follows:

$$\hat{P}^{(\varepsilon)}(\tau) = \frac{\sum_{i=1}^{N-\tau} \Theta(\varepsilon - \|\mathbf{x}_i - \mathbf{x}_{i+\tau}\|)}{N - \tau} = \frac{\sum_{i=1}^{N-\tau} R_{i,i+\tau}^{(\varepsilon)}}{N - \tau}. \quad (2)$$

$\hat{P}^{(\varepsilon)}(\tau)$  is a generalized autocorrelation function, as it also describes higher-order correlations between the points of the trajectory in dependence on  $\tau$ . A further advantage with respect to the linear autocorrelation function is that  $\hat{P}^{(\varepsilon)}(\tau)$  is determined for a trajectory in phase space and not only for a single observable of the system's trajectory. (From now on, we omit  $(\varepsilon)$  and  $\hat{\cdot}$  in  $\hat{P}^{(\varepsilon)}(\tau)$  to simplify the notation.) In contrast to a periodic system, for chaotic oscillators, the probability that the trajectory recurs after one oscillation is less than 1. For example, for two coupled Rössler oscillators<sup>(1)</sup> in phase-coherent regime, strong local maxima occur at multiples of the mean period of the chaotic system. One also observes in the periodically driven Lorenz system [20] local maxima in  $P(\tau)$  in the phase-synchronized case. However, these local maxima are smaller and broader than in the case of two coupled Rössler systems. This reflects the effective noise intrinsic in the Lorenz system, *i.e.* the switchings between the two lobes of the attractor which occur rather irregularly. Thus, we have imperfect phase synchronization [20] and an exact frequency locking between the periodic forcing and the Lorenz system cannot be observed. As we consider PS in a statistical sense by means of  $P(\tau)$ , we can detect synchronization also in this case without making a projection of the attractor beforehand. Looking at the coincidence of the positions of the maxima of  $P(\tau)$  for both coupled systems, we can quantitatively identify PS. Therefore, we introduce the cross correlation coefficient between  $P_1(\tau)$  and  $P_2(\tau)$  to quantify PS:

$$CPR = \langle \bar{P}_1(\tau) \bar{P}_2(\tau) \rangle / (\sigma_1 \sigma_2), \quad (3)$$

where  $\bar{P}_{1,2}$  means that the mean value has been subtracted and  $\sigma_1$  and  $\sigma_2$  are the standard deviations of  $P_1(\tau)$ , respectively  $P_2(\tau)$ . If both systems are in PS, the probability of recurrence is maximal at the same time and  $CPR \sim 1$ . In contrast, if the systems are not in PS, the maxima of the probability of recurrence do not occur simultaneously. Then we observe a drift and hence expect low values of  $CPR$ . This method yields good results even for non-phase-coherent oscillators, such as the two mutually coupled Rössler systems in the funnel regime (figs. 1a, b), where the direct application of the conventional methods is not appropriate [14]. In this case, the peaks in  $P(\tau)$  are now not as well pronounced as in the phase-coherent case (figs. 1c, d). This reflects the different time scales that come into play or the broad-band power spectrum in the funnel system. However, we see that for non-PS ( $\mu = 0.05$ ) the positions of the local maxima do not coincide (fig. 1c), whereas for PS ( $\mu = 0.2$ ) the locations of the local maxima coincide for both oscillators (fig. 1d). Furthermore, we can detect PS even in time series corrupted by noise. We consider two coupled Rössler systems in phase-coherent regime. We add a realization of colored noise with a very high noise amplitude to each component of the first system and another realization of colored noise with a smaller noise amplitude to each component of the second system (figs. 1e, f). The method presented in [14] is not appropriate to estimate the phase in this case, because it requires the computation of the derivative of the time series, and due to the large level of noise, this is not possible. But by means of  $P(\tau)$  we can distinguish PS from non-PS even in this case (figs. 1g, h). Additionally, the RP-based synchronization index indicates clearly the onset of PS. In the coherent case, the  $CPR$  index increases strongly at  $\mu = 0.037$ , indicating the transition to PS (fig. 2a),

<sup>(1)</sup>The equations are the following:  $\dot{x}_{1,2} = -\omega_{1,2}y_{1,2} - z_{1,2}$ ,  $\dot{y}_{1,2} = \omega_{1,2}x_{1,2} + ay_{1,2} + \mu(y_{2,1} - y_{1,2})$ ,  $\dot{z}_{1,2} = 0.1 + z_{1,2}(x_{1,2} - 8.5)$ .

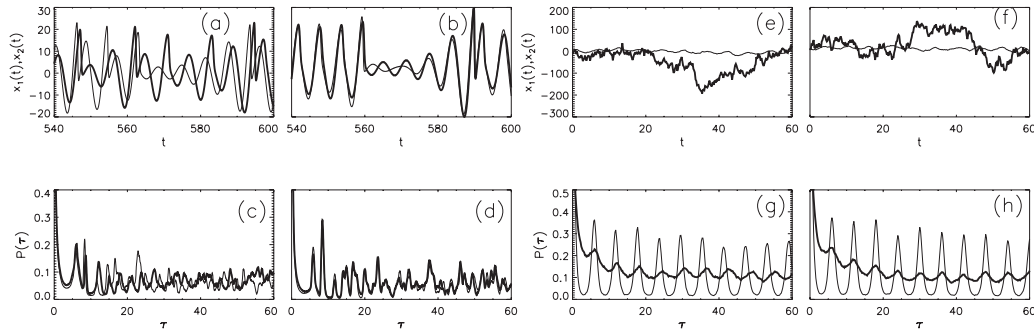


Fig. 1 – (a), (b) Segments of the  $x$ -components of the trajectories of two mutually coupled Rössler systems in non-phase-coherent (funnel) regime ( $a = 0.2925$ ); (a) for  $\mu = 0.05$  (non-PS), (b) for  $\mu = 0.2$  (PS). (c)  $P(\tau)$  for the two funnel Rössler for  $\mu = 0.05$  (non-PS). (d)  $P(\tau)$  for the two funnel Rössler for  $\mu = 0.2$  (PS). (e), (f) Segments of the  $x$ -components of the trajectories of two mutually coupled Rössler systems in phase-coherent regime ( $a = 0.16$ ) strongly contaminated by colored noise. A realization of  $r_{t+1} = 0.99r_t + 10\eta_t$  and  $s_{t+1} = 0.982s_t + \xi_t$  were, respectively, added to each component of the Rössler systems. (e) non-PS ( $\mu = 0.02$ ). (f) PS ( $\mu = 0.05$ ). (g)  $P(\tau)$  for the two noisy Rössler for  $\mu = 0.02$  (non-PS), (h)  $P(\tau)$  for the two noisy Rössler for  $\mu = 0.05$  (PS). Solid line: system 1, dashed line: system 2.

which coincides with the transition of the fourth Lyapunov exponent  $\lambda_4$  to negative values (fig. 2e), as expected. In the non-coherent case,  $\lambda_4$  has already passed to negative values for  $\mu > 0.02$  (fig. 2f). However,  $CPR$  (fig. 2b) is still rather low: it does not reveal the transition to PS until approximately  $\mu = 0.18$ . This coincides with the transition of  $\lambda_2$  from positive values to zero (fig. 2f), indicating the establishment of a strong correlation between both oscillators. Because of the non-coherency of the oscillators, a higher coupling strength is needed to synchronize them [14].

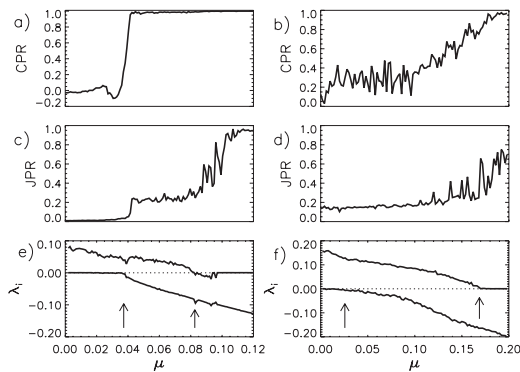


Fig. 2

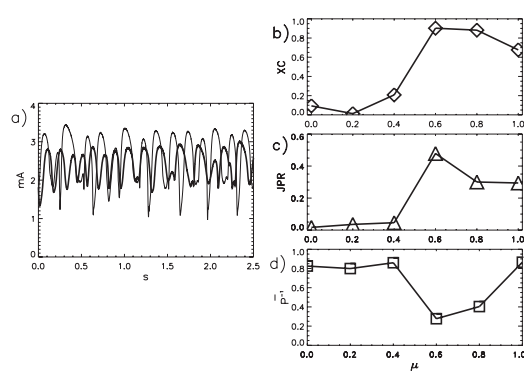


Fig. 3

Fig. 2 –  $CPR$  index,  $JPR$  index and  $\lambda_2$  and  $\lambda_4$  as functions of the coupling strength  $\mu$  for two mutually coupled Rössler systems in phase-coherent regime (a,c,e) and in funnel regime (b,d,f). The dotted zero line in (e) and (f) is plotted to guide the eye. Here, we choose  $\varepsilon$  corresponding to 10% recurrence points in each RP.

Fig. 3 – a) Current of two non-coherent electrochemical oscillators in dependence on time for coupling strength  $\mu = 0$ . b)  $XC$  index for PS, c)  $JPR$  index for GS, d)  $\bar{P}^{-1}$  index for GS (method of mutual false nearest neighbors). All these indices are represented in dependence on the coupling strength for the non-phase-coherent electrochemical oscillators.

The results obtained with *CPR* are very robust with respect to the choice of the threshold  $\varepsilon$ . Simulations show that the outcomes are almost independent of the choices of  $\varepsilon$  corresponding to a percentage of black points in the RP between 1% and 90%, even for non-coherent oscillators. The details of the recurrence structures in the RP are of course dependent on the choice of  $\varepsilon$ . Choosing  $\varepsilon$  for both interacting oscillators, in such a way that the percentage of black points in both RPs is the same, the relationship between their respective recurrence structures does not change for a broad range of values of  $\varepsilon$ .

*Detection of GS.* – Now we show that it is also possible to detect GS by means of the RP method. Two systems  $\mathbf{x}$  and  $\mathbf{y}$  are said to be generalized synchronized if a relationship  $\mathbf{y}(t) = \mathbf{f}(\mathbf{x}(t))$  holds [2–4]. When the system equations are known, GS can be characterized by the conditional stability of the driven chaotic oscillator [3]. However, dealing with measured time series, the model equations are usually not known. Hence, several methods based on the technique of delay embedding and on the conditional neighbors have been developed to characterize GS, such as the method of mutual false nearest neighbors (MFNN) [2, 4, 21]. But systems exhibiting non-invertibility and/or wrinkling hamper the detection of GS by such techniques [22]. Further techniques, such as the  $\delta^p$  and  $\delta^{p,q}$  method, have been developed to overcome these problems [23]. We define an index for GS based on RPs that also overcomes these problems. It is based on the result presented in [17, 18]: only considering the recurrence matrix of a trajectory, is it possible to reconstruct topologically the trajectory in phase space. Hence, two systems connected by a functional relationship have the same recurrence matrix. Let us consider the average probability of recurrence over time, which is given by  $RR^{\mathbf{x}} = \frac{1}{N^2} \sum_{i,j=1}^N \Theta(\varepsilon_{\mathbf{x}} - \|\mathbf{x}_i - \mathbf{x}_j\|)$  (analogously for  $\mathbf{y}$ ). Then, the average probability of joint recurrence over time [24] is given by  $RR^{\mathbf{x},\mathbf{y}} = \frac{1}{N^2} \sum_{i,j=1}^N \Theta(\varepsilon_{\mathbf{x}} - \|\mathbf{x}_i - \mathbf{x}_j\|) \Theta(\varepsilon_{\mathbf{y}} - \|\mathbf{y}_i - \mathbf{y}_j\|)$ . If both systems  $\mathbf{x}$  and  $\mathbf{y}$  are independent of each other, the average probability of a joint recurrence is given by  $RR^{\mathbf{x},\mathbf{y}} = RR^{\mathbf{x}} RR^{\mathbf{y}}$ . If the oscillators are, on the other hand, in GS, we expect an approximate identity of their respective recurrences, and hence  $RR^{\mathbf{x},\mathbf{y}} \simeq RR^{\mathbf{x}} = RR^{\mathbf{y}}$ . For the computation of the recurrence matrices in the case of essentially different systems that undergo GS, it is more appropriate to use a fixed number of nearest neighbors  $N_N$  for each column in the matrix [21] than using a fixed threshold. Hence, the  $\varepsilon^i$  are different for each column in their respective RPs, but subjected to the following condition:  $\sum_{j=1}^N \Theta(\varepsilon_{\mathbf{x}}^i - \|\mathbf{x}_i - \mathbf{x}_j\|) = N_N \forall i$  (analogously for  $\mathbf{y}$ ).  $RR^{\mathbf{x}}$  and  $RR^{\mathbf{y}}$  are then equal and fixed by  $N_N$ , because  $RR^{\mathbf{x}} = RR^{\mathbf{y}} = N_N/N$ . We call  $RR = N_N/N$ . Hence, the coefficient  $S = \frac{RR^{\mathbf{x},\mathbf{y}}}{RR}$  is an index for GS that varies from  $RR$  (independent) to 1 (GS). However,  $S$  does not indicate LS. For this reason, we include a time lag in the similarity  $S(\tau) = \frac{\frac{1}{N^2} \sum_{i,j} \Theta(\varepsilon_{\mathbf{x}}^i - \|\mathbf{x}_i - \mathbf{x}_j\|) \Theta(\varepsilon_{\mathbf{y}}^i - \|\mathbf{y}_{i+\tau} - \mathbf{y}_{j+\tau}\|)}{RR}$ , where the thresholds  $\varepsilon_{\mathbf{x}}^i$  and  $\varepsilon_{\mathbf{y}}^i$  are chosen in such a way that the number of nearest neighbors for each column is equal to  $N_N$ . Then, we choose the maximum value of  $S(\tau)$  and normalize:

$$JPR = \max_{\tau} \frac{S(\tau) - RR}{1 - RR}, \quad (4)$$

which is based on the average joint probability of recurrence.  $JPR$  ranges from 0 to 1.  $RR$  is a free parameter. However, simulations show that the  $JPR$  index is rather independent of the choice of  $RR$ . In the simulations shown here we use  $RR = 0.1$ . Now we apply  $JPR$  to two Rössler oscillators in coherent and non-coherent regime. In the coherent case, the index  $JPR$  in dependence on the coupling strength  $\mu$  shows three plateaus (fig. 2c). The beginning of the third plateau indicates the onset of LS because it becomes nearly one at approximately  $\mu = 0.1$ . This occurs shortly after the zero crossing of  $\lambda_2$ , at  $\mu = 0.08$  (fig. 2e). Between

$\mu = 0.08$  and  $\mu = 0.1$  the values of  $JPR$  have large fluctuations. This reflects the intermittent LS, where LS is interrupted by intermittent bursts [7,8]. In the non-coherent case  $JPR$  reaches rather high values at  $\mu \sim 0.17$  (fig. 2d), indicating the onset of GS. This coincides with the zero crossing of  $\lambda_2$  (fig. 2f). Note that we have detected GS almost simultaneously with PS (fig. 2b), which is a typical characteristic for non-coherent oscillators [14]. Furthermore, we have analyzed by  $JPR$  the non-invertible and wrinkling maps presented in [22,23]. In these cases, we have found that embedding both the driver and response signals before computing the index  $JPR$  facilitates the detection of GS, as proposed in [23]. Using an embedding dimension of 8 for both the driver and response signal, we could detect GS in all cases.

*Application to chaotic electrochemical data.* – In order to test the applicability of the method to experimental data, we analyze time series from two coupled electrochemical oscillators (fig. 3d). The experiments were done with electro-dissolution of iron in sulfuric acid in which non-phase-coherent chaotic signals can be obtained and in which coupling strength can be varied [25]. From computing  $CPR$  and  $JPR$  for different coupling strengths  $\mu = \{0.0, 0.2, 0.4, 0.6, 0.8, 1.0\}$ , we detect the transition to PS and GS simultaneously at the coupling strength  $\mu = 0.6$  (fig. 3), in accordance with theoretical results [14]. In contrast, the method of mutual false nearest-neighbors (MFNN) [2–4] does not yield plausible results in this case. The index  $\bar{P}^{-1}$  is the inverse of the mean value of the MFNN parameter. This index is zero for systems that are not in GS, and approximately one for systems in GS [2–4]. We observe in fig. 3d that for no coupling ( $\mu = 0$ ) the index  $\bar{P}^{-1}$  indicates GS, and for coupling strength  $\mu = 0.6$ , where the other two indices  $CPR$  and  $JPR$  indicate synchronization (figs. 3b, c),  $\bar{P}^{-1}$  does not. Hence, in the case of non-coherent oscillators the method of MFNN does not yield reliable results<sup>(2)</sup>.

Now we regard the more complicated case of non-stationary data, where the non-stationarity is imposed through a linear continuous change of a controllable parameter, the applied potential. In this case we consider two different values of the coupling strength:  $\mu = 0.0$  and  $\mu = 0.6$ . The recurrence-based method does not demand stationarity to the data set to be analyzed [16]. Hence, we can apply both indices for PS and GS to the whole data set without preprocessing the time series. For coupling strength  $\mu = 0$ , we get  $CRP = 0.0946$  and  $JPR = 0.0121$ , indicating the absence of PS, respectively GS, as expected. For coupling strength  $\mu = 0.6$  we obtain  $CPR = 0.846$ , which is a strong indication for the presence of PS. Additionally, we yield  $JPR = 0.202$  for this  $\mu$ , which is one order of magnitude larger than the value obtained for  $\mu = 0$ . This is an indication for the presence of GS.

Furthermore, we have performed numerical simulations, where we have added different trends (linear, periodic and non-linear) to one of the oscillators in the models considered above. In all these cases one can clearly discern by means of  $P(\tau)$  between PS, GS and no synchronization at all. This is due to the fact that there is no need to choose an origin, around which the system oscillates. Hence, it does not matter if the “origin” wanders with time (by the definition of the phase based on the Hilbert transformation, difficulties appear with non-stationary time series, as the center of rotation varies with time [5, 6]). Also by adding large amounts of observational noise to the oscillators, it is still possible to detect PS with the proposed statistical measure. This robustness against noise is due to the fact that we do not consider the coincidence of local recurrence patterns, but average ones.

*Conclusions.* – In conclusion, we have presented a new method to detect PS and GS (including LS) of chaotic systems based on the idea of recurrences in phase space, as demonstrated

---

<sup>(2)</sup>We used a total of 25000 data points,  $T_r = T_d = 0.035$  s (the sampling rate was 2 kHz),  $d_r = 5$  and  $d_d = 12$ . We computed  $P(n, d_r, d_d)$  at 10000 different locations on the attractor and used them to evaluate the average values  $\bar{P}(d_r, d_d)$ .



for model systems and experimental data. This technique has several advantages with respect to other methods proposed so far: i) it enables the detection of PS and GS even for rather complex and non-phase-coherent cases and in experimental data, even when they are subjected to non-stationarities; ii) it is possible to detect and quantify PS and GS with the same method. Applications of this approach seem to be very promising to experimental data in which the explicit computation of the phase is controversial and where non-stationarity is often a concern, *e.g.*, physiological or geophysical data. The generation of appropriate surrogates to test the significance of the obtained results is still an important open problem, that has to be addressed.

\* \* \*

We thank C. ZHOU, G. OSIPOV, M. ROSENBLUM and M. ZAKS for useful discussions and QING LV for help with the experiments. This work was supported in part by the National Science Foundation under grant CTS-0317762, the “DFG priority program 1114” and “Helmholtz Center for Mind and Brain Dynamics”.

#### REFERENCES

- [1] PECORA L. M. and CARROLL T. L., *Phys. Rev. Lett.*, **64** (1990) 821.
- [2] RULKOV N. F., SUSHCHIK M. M., TSIMRING L. S. and ABARBANEL H. D. I., *Phys. Rev. E*, **51** (1995) 980.
- [3] KOCAREV L. and PARLITZ U., *Phys. Rev. Lett.*, **76** (1996) 1816.
- [4] BOCCALETTI S., VALLADARES D. L., KURTHS J., MAZA D. and MANCINI H., *Phys. Rev. E*, **61** (2000) 3712.
- [5] ROSENBLUM M. G., PIKOVSKY A. S. and KURTHS J., *Phys. Rev. Lett.*, **76** (1996) 1804.
- [6] PIKOVSKY A. S., ROSENBLUM M. G. and KURTHS J., *Synchronization* (Cambridge Nonlinear Science Series 12) 2001.
- [7] ROSENBLUM M. G., PIKOVSKY A. S. and KURTHS J., *Phys. Rev. Lett.*, **78** (1997) 4193.
- [8] SOSNOVTSEVA O. V., BALANOV A. G., VADIVASOVA T. E., ASTAKHOV V. V. and MOSEKILDE E., *Phys. Rev. E*, **60** (1999) 6560.
- [9] BLASIUS B., HUPPERT A. and STONE L., *Nature*, **399** (1999) 354.
- [10] TASS P., ROSENBLUM M. G., WEULE J., KURTHS J., PIKOVSKY A. S., VOLKMANN J., SCHNITZLER A. and FREUND H.-J., *Phys. Rev. Lett.*, **81**(15) (1998) 3291.
- [11] ROSENBLUM M. G., CIMPONERIU L., BEZERIANOS A., PATZAK A. and MROWKA R., *Phys. Rev. E*, **65** (2002) 041909.
- [12] DESHAZER D. J., BREBAN R., OTT E. and ROY R., *Phys. Rev. Lett.*, **87**(4) (2001) 044101.
- [13] ROSENBLUM M. G., PIKOVSKY A. S., KURTHS J., OSIPOV G. V., KISS I. Z. and HUDSON J. L., *Phys. Rev. Lett.*, **89** (2002) 264102.
- [14] OSIPOV G. V., HU B., ZHOU C., IVANCHENKO M. V. and KURTHS J., *Phys. Rev. Lett.*, **91** (2003) 024101.
- [15] POINCARÉ H., *Acta Math.*, **13** (1890) 1.
- [16] ECKMANN J.-P., KAMPHORST S. O. and RUELLE D., *Europhys. Lett.*, **4** (1987) 973.
- [17] THIEL M., ROMANO M. C. and KURTHS J., *Phys. Lett. A*, **330** (2004) 343.
- [18] THIEL M., ROMANO M. C., KURTHS J. and READ P., *Chaos*, **14** (2004) 234.
- [19] THEILER J., *Phys. Rev. A*, **34** (1986) 2427.
- [20] ZAKS M. A., PARK E.-H. and ROSENBLUM M. G., *Phys. Rev. Lett.*, **82** (1999) 4228.
- [21] ARNHOLD J., GRASSBERGER P., LEHNERTZ K. and ELGER C. E., *Physica D*, **134** (1999) 419.
- [22] SO P., BARRETO E., JOSIC K., SANDER E. and SCHIFF S. J., *Phys. Rev. E*, **65** (2002) 046225.
- [23] HE D., ZHENG Z. and STONE L., *Phys. Rev. E*, **67** (2003) 026223.
- [24] ROMANO M. C., THIEL M., KURTHS J. and VON BLOH W., *Phys. Lett. A*, **330** (2004) 214.
- [25] KISS I. Z., LV Q. and HUDSON J. L., *Phys. Rev. E*, **71** (2005) 035201(R).